Vol. 55: 65–78, 2012
doi: 10.3354/cr01113

CLIMATE RESEARCH
Clim Res

Published November 15

Effect of temporal and spatial scales of weather data on crop yield forecasts

Sanai Li, Adrian M. Tompkins*

Earth System Physics Section, The Abdus Salam ICTP, Trieste, Italy

ABSTRACT: A dynamical crop model is used to understand the statistical relationship between climate and wheat yield in China. Using 16 years of regional yield data and a gridded database of climate data, it is shown that a clear statistical relationship is lacking in many points between seasonal mean climate anomalies and yield. Dynamical simulations of yield using daily climate data to drive the crop model demonstrate that this is partly due to the strongly nonlinear relationship between climate and yield, which can thus hamper the application of linear statistical models for forecasting and planning purposes. A case study using individual station data emphasized how local variations in climate could be substantial, and could have marked effects on simulated yields. Due to the memory effect of the soil moisture, little difference was found when driving the crop model with 5 d (pentad) temporally averaged rainfall data. This result is relevant for crop studies, as reliable pentad satellite-based rainfall retrievals are available for a far longer period than daily data. The highly skewed distribution of rainfall implies 10 d or longer averaging of rainfall strongly impacts crop yield, although temperature, a spatially smoother field, could be averaged for dekads or even monthly. Spatially averaging the driving climate data shows that the crop model skill in yield forecasting improves as the spatial scale of weather data increased from 2° × 2° to 0.5° × 0.5°, even if point-wise sampling errors are greater.

KEY WORDS: Dynamical crop model · Temporal and spatial scale · Crop forecasting

1. INTRODUCTION

Crop yield monitoring and timely predictions on regional, national and pan-national scales are receiving increased attention in both developing and developed countries to aid farmers and decision makers (Bouman et al. 1995). Interannual variability in yield is driven by a wide range of factors, including socioeconomic drivers of crop demand, land use change, governmental and non-governmental organization intervention programmes (such as fertilizer subsidies), technology improvements, population migration, pests and diseases. Crop yield fluctuations are also affected by climate anomalies in temperature, solar radiation and precipitation, especially in regions of rain-fed agriculture. Extreme climate events, such as high temperature stress, drought and flooding, could result in a severe reduction in agricultural production. The responses of crop yield to climate variability vary widely among regions, depending on the cropping system and climate (Li. et al. 2010a). Understanding how climate affects crop yield can aid in the development of monitoring and prediction tools, consequently help planners and farmers to take advantage of favorable climate, and reduce negative effects (Jones et al. 2000). Relative to uncertain socioeconomic conditions and management decisions adopted by small-scale farm households, climate variables are to a certain degree more readily measurable and are monitored through various operational real-time weather analyses (e.g. Dee et al. 2011) and ultimately are predictable with varying leadtimes.

One simple method to monitor (and ultimately predict) crop growth is to use weather observations (fore-

*Corresponding author. Email: tompkins@ictp.it

casts) to drive crop models from local to continental scales (Nemecek et al. 1996, Thornton et al. 1997, Challinor et al. 2004, Hansen et al. 2004). The crop model can be either statistical or dynamical. The statistical models predict yield using previously observed empirical relationships between climate and yield. These models are often the preferred method for crop forecasting due to their low data requirements and simplicity to implement (Becker-Reshef et al. 2010). However, statistical regression models are limited by the non-linear response of crops to their environments (in particular, weather) (Semenov & Porter 1995, Porter & Semenov 1999, 2005) and by the relatively short data records in many developing countries.

In contrast, dynamic crop models seek to explicitly simulate crop growth and development and its response to environmental variables. The potential advantage of a dynamical crop model working with a daily timestep is the ability to account for the influence of sub-seasonal climate variability on crop yield. They can represent the strong nonlinearity of the relationship between weather and yield, in particular for extreme events. However, the dynamical models are limited by the accuracy of their representation of the physics itself and uncertainty in key parameter settings, such as the algorithm employed to determine planting date for example in the General Large Area Model for crops (GLAM): when available soil water meets a threshold of requirement, then the crop is sown (Challinor et al. 2004). The potential success of the crop yield monitoring system depends on the climate observations, agricultural statistics and the accuracy of the crop modeling tools themselves. Crop forecast accuracy is also affected by forecast scale (Bezuidenhout & Singels 2007).

The temporal scale of temperature and rainfall is important in determining crop yield. Critical temperature thresholds often have to be exceeded for several consecutive days for significant plant damage (Challinor et al. 2005), and sub-seasonal rain breaks are only likely to have an impact if on the order of 1 wk or more. This question is important since shorter timesteps imply much greater random errors on a satellite rainfall product or likewise for the sampling error of raingauge measurements. Daily rainfall products from satellite are only available from approximately the last decade (e.g. 1997 for Global Precipitation Climatology Project [GPCP], Huffman et al. 1995; and 2003 for CPC morphing technique [CMORPH], Joyce et al. 2004). Before this period, the reliance on infrared intensity temperature measurements meant that heavy temporal averaging was required to reduce point measurements to an acceptable level; this is the reason why the Tropical Applications of Meteorology Using Satellite Data (TAMSAT) precipitation estimates are currently only available as 10 d dekadal averages (Grimes et al. 1999, Thorne et al. 2001), and common global products such as CMAP (Climate Prediction Center [CPC] Merged Analysis of Precipitation) and GPCP are only available as monthly means or pentad (5 d mean) products during the 1980s and 1990s (Huffman et al. 1995, Xie & Arkin 1997). In the same way, the representativeness of a raingauge measurement increases when averaged over time (Ciach 2003, Bowman 2005, Villarini et al. 2008). These random errors would not be important if the crop yield was not such a strong nonlinear function of the driving climatic variables.

The choice of spatial variability involves similar issues. Running a dynamical model on a finer spatial grid can take advantage of the improved resolution of recent satellite products for model rainfall, radiation and land use to correctly define farmed areas within a district. Olesen et al. (2000) showed that employing the finest resolution of soil and climate data gave a better fit of simulated to observed spatial autocorrelation in yield, and Easterling et al. (1998) found that agreement between simulated and observed crop yield in Niger was greatly improved when climate data was disaggregated from a large scale to ~1° × 1° resolution, due to improved frequency and intensity statistics of rainfall. Previous work has indicated an upper limit to the improvement gained by resolution, however, and Easterling et al. (1998) found no further improvement while disaggregating climate data to scales finer than the 1° × 1° resolution. One possible reason for this could be the inaccuracy of observed yields at small scales (finer than 1° × 1° resolution), which suffer from random errors or unmeasurable confounding factors, such as spatial variability in biological and human controls including pest, pathogen outbreaks and management.

It is apparent from the above discussion that there may exist a clear scale separation between the climate-related drivers of yield variability, which in particular for drought can be assumed to operate on a coherent regional scale (Hannaford et al. 2011), in contrast to random errors in yield statistics that are likely to occur at smaller district spatial scales. The small spatial scale of the random error component is evident when examining a map of crop yield (Sudduth & Drummond 2007). Such random errors would average out over larger scales. This points to the possibility of developing spatial filters to remove or correct erroneous yield data reports and reveal the wider climate-forced signal. In contrast, pest out-

breaks and management decisions are confounding factors that are likely to be intertwined and driven partly by climate factors and thus potentially operate over similar spatial scales, acting as a positive or negative feedback, respectively, to the raw climate-driven yield variability.

The objectives of this study are to use a dynamical crop model for wheat to (1) analyse the correlation between wheat yield, rainfall and temperature to understand how observed and simulated yield respond to climate variables in the area of study; (2) investigate how the temporal average of rainfall and temperature affect the ability of crop models to forecast yield, especially the impact of the sub-pentad variability of rainfall on crop yield; (3) find the appropriate spatial scales of weather data needed for a crop model to improve forecast accuracy; and (4) assess if a simple filtering of small spatial scale crop yield anomalies can improve the crop yield forecast by more clearly identifying the climate signal.

2. MATERIALS AND METHODS

2.1. Research area

The major wheat planting areas of China were selected to assess the spatial resolution sensitivity of a dynamical crop model. China was chosen as the study region for a number of reasons. The large size of the country implies a relatively uniform methodology for collecting yield statistics across a wide range of diverse climatic zones, avoiding the frequently problematic discreteness of yield data when crossing national boundaries. Relative to many countries that still have widespread rainfed and irrigated agriculture, China has a long record of data for both climate and crops.

In order to evaluate the effect of using different temporal average weather data and daily weather data on the simulation of wheat yield, 6 sites in China —Guyuan, Guyang, Huma, Hefei, Zhengzhou and Beijing (Table 1)— were chosen as case studies. These 6 sites represent different climatology and geography. Guyuan, Guyang and Beijing are in the semi-arid regions with average seasonal total rainfall in the range of 181 to 267 mm from 1980 to 1999. Huma, Zhengzhou and Hefei are semi-humid regions with average seasonal total rainfall in the range of 209 to 477 mm from 1980 to 1999. Guyuan, Guyang and Huma are the major spring wheat producing areas, while Beijing, Zhengzhou and Hefei are major winter wheat planting areas.

Table 1. Details of the 6 sites in China for 1985–1999 used in this study. *R*: seasonal total rainfall, *T*: seasonal mean temperature

Locations	°N	°E	Rain (mm)	SD of *R* (mm)	*T* (°C)	SD of *T* (°C)
Guyang	41.03	110.05	172	51	18.6	0.63
Guyuan	36.00	106.27	233	41	15.5	0.51
Huma	51.72	126.65	303	93	17.6	0.7
Beijing	39.33	116.28	136	67	6.9	0.44
Zhengzhou	34.24	113.22	209	72	9.1	0.5
Hefei	31.01	117.28	477	111	10.7	0.34

2.2. Weather data

The 0.5° × 0.5° daily minimum/maximum temperature and rainfall (called CN05) are available from the China Meteorological Administration (CMA). A 0.5° × 0.5° daily minimum and maximum temperature for 1961 to 2005 was derived by merging the climatology and Angular Distance Weighting interpolated anomalies from 751 observing stations in China (see Fig. 1 in Xu et al. 2009). The 0.5° × 0.5° daily precipitation dataset from 1978 to 2003 was developed by Xie et al. (2007) over China, based on ~700 meteorological stations before 2003 and over 1000 hydrological stations in the Yellow River basin before 1997. The gauge network is quite dense over eastern China with inter-gauge distances on the order of 10 km, while over western China the station density is lower. Few stations are found over the northwestern part of the Tibetan Plateau. Random sampling errors decrease with increasing gauge network density (Xie et al. 2007, Xu et al. 2009).

Incoming solar radiation are from short range forecasts starting from ERA-40 (ECMWF 40 Year Reanalysis) for 1985 to 1988 and from ERA-interim for 1989 to 2000. The values of 0.5° incoming solar radiation are disaggregated from 1.25° ERA-40 and 0.75° ERA-interim data. In order to evaluate the impact of input weather at different spatial scales on crop simulation, 1° × 1° and 2° × 2° weather data were obtained by aggregating 0.5° × 0.5° weather data. Then, 0.5°, 1° and 2° daily weather data are respectively used as inputs to the GLAM crop model from 1985 to 2000 over China.

2.3. Crop data

Wheat is the second most important food crop in China in terms of both planting area and production. From 1985 to 2000, wheat planting area accounted

for 24.5 to 27.5% of China's total food crop area (CSY 2001). The county level wheat yield data (spring and winter wheat combined) were calculated from the wheat plantation area and production data, which are available from the CMA. The spatial distribution of the spring wheat (mainly planted in northeast and northwest China) and winter wheat (mainly planted in the North China Plain [NCP], southeast and southwest China) planting regions in China can be seen in Fig. 1. The wheat plantation area is divided into spring wheat and winter wheat areas, based on wheat agro-ecological production zones in China (He et al. 2001). The growing season for spring wheat is normally from April to September, and October to May for winter wheat. China itself is divided into 5 main regions: the North China Plain, Northeast, Northwest, Southwest, and Southeast (Fig. 1).

In most of the NCP, the crop irrigation fraction is between 40 to 80% (crop irrigation fractions are from the global map of irrigated areas: www.fao.org/geonetwork/srv/en/main.home). In northeast and southeast China, crops are only partly irrigated, and irrigation accounts for around 0 to 20%. In the Southwest and Northwest provinces, irrigation accounts for a small percentage and even no irrigation in some areas (Fig. 2). Accurate irrigation data for the wheat crop, in terms of fractional area and irrigation strategy, was not available for this study, and thus irrigation is not accounted for.

Wheat yields at the county level were aggregated into 0.5° scale yields by ArcGIS to match the gridded weather data. The area of counties varies from 56 to 270 000 km^2. The yield trend in the grid cells was approximated using a best fit third-order polynomial equation, which was then used to detrend the yield data for technology advances to match 1985 levels. Then the detrended yields in the major agriculture grids were spatially aggregated to regions (as marked in Fig. 1) to examine the performance of GLAM with different scales in weather input at the regional level.

2.4. Model description

The dynamical model used in the study is the GLAM, which has been designed to operate at the spatial scale of global and regional climate models. GLAM is a process-based regional crop model with daily time step simulation. The model simulates the soil water balance, leaf canopy and root growth, biomass and yield production, which are limited by a yield gap parameter (YGP), inadequate soil water or extremes in temperature. The model was originally designed for groundnut, and has been successfully used to simulate yields over large areas in India (Challinor et al. 2004). A more recent development was the application of the model to predict wheat yields (Li et al. 2007), with Li et al. (2010b) reporting a good agreement between simulated and observed wheat yields at a regional level in China.

In all versions of the model, yield predictions must be preceded by a calibration stage. The input parameters range was obtained from the literature and then calibrated by observations. The crop-specific parameters of GLAM for wheat have been calibrated using the observations by Li (2008). A site-specific parameter is used to calibrate the model by setting the value of the YGP, using an ensemble integration

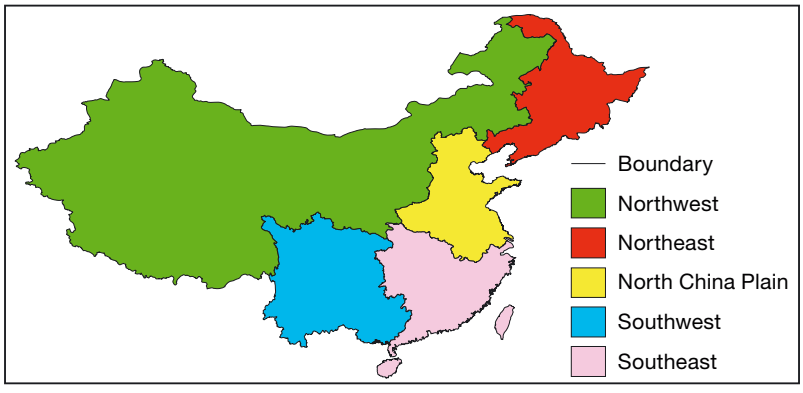

Fig. 1. Principal regions in China

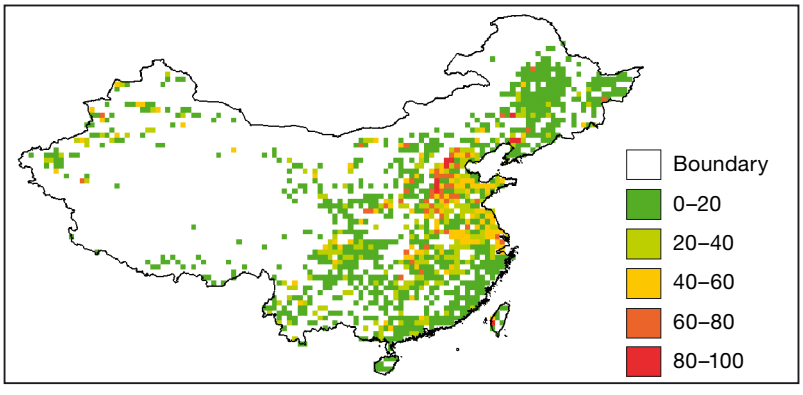

Fig. 2. Percentage (%) of crop irrigation area from 1990 to 2000

conducted for a number of years to compare the predicted yields to observations. The YGP decreases the yield from the theoretical maximum to the long-term average observed value in order to account for pests, management strategies and other confounding factors. The optimal value of the YGP in each grid cell was chosen by minimizing root mean square error (RMSE) between observed and simulated yields for 2 periods: 1985–1990 and 1991–2000.

The inputs used by GLAM are daily maximum and minimum temperatures (°C), precipitation (cm), solar radiation (MJ m^{-2} d^{-1}), soils texture types and sowing date. In order to assess how the temporal scale of climate data affects the forecast ability of the crop model, the GLAM is driven by daily, 5, 10 and 30 d average rainfall and temperature, respectively, in the representative sites in China. Daily data is averaged and re-converted from 5, 10 and 30 d average rainfall and temperature data. The dominant agricultural soil texture types are based on the FAO digital world soil map (Batjes 1997), and are aggregated to the 0.5° × 0.5° grid using ArcGIS. The wheat sowing windows were taken from the plant sowing data map of China (Cui et al. 1983), which were interpolated to the grid by the inverse distance weighted methods. Sowing dates are determined by the local calendar and condition of soil moisture. In GLAM, when available soil water meets a threshold of requirement within the sowing windows (30 d), the crop is sown.

The respective correlations between the growing seasonal mean temperature, total amount of precipitation, and observed and simulated wheat yield at the 0.5° scale were analysed in order to determine the main climate factors influencing the inter-annual variation in yield. The response of simulated wheat yields to temperature and rainfall were examined and compared with the measured responses from observations. Compared to yield variability due to the seasonal mean climate anomalies, extreme climatic events (such as floods and droughts) can have a more dramatic impact on crop yield, implying that the yield–climate relationship is likely to be highly nonlinear.

3. RESULTS AND DISCUSSION

3.1. The statistical relationship between wheat and climate

3.1.1. Observations

The statistical correlation between wheat yield and seasonal weather anomalies (April to September for spring wheat and October to May for winter wheat) from 1985 to 2000 are shown in Fig. 3. The striking aspect of these correlation plots (Fig. 3) is that 54 % of grid cells show no statistical relationship ($p > 0.1$) between weather and yield at all, implying that prediction based on a linear statistical approach would likely fail. For this period, observed wheat yield anomalies are significantly correlated with growing seasonal total rainfall or seasonal mean temperature in 569 out of 1238 grid cells, and even where a statistically significant relationship does exist ($p < 0.1$), the regions are highly spatially variable, and the correlation can be of both signs.

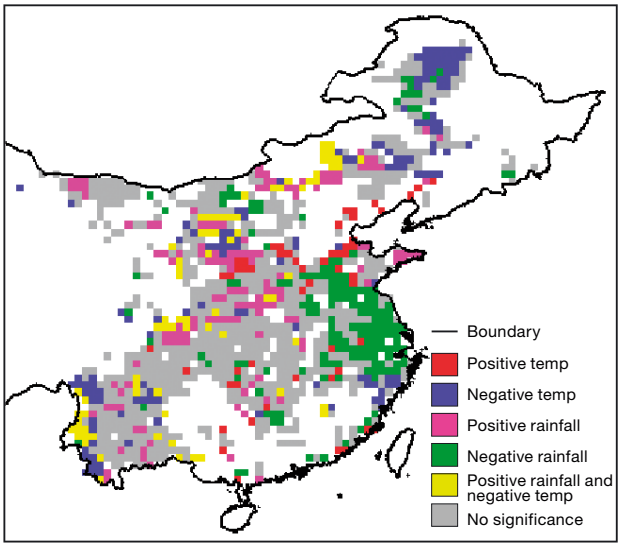

Fig. 3. Dominant rainfall and temperature relationships with inter-annual variability of wheat yield using temperature, rainfall and observed yield data at the 0.5° scale in China from 1985 to 2000 (Apr–Sep for spring wheat and Oct–May for winter wheat)

As discussed in the introduction, there are many factors that may confound the attempt to determine seasonal mean yield–climate relationships. Climate variability on a sub-seasonal timescale may be more important for crops than seasonal mean totals, and more generally, climate drivers of yield may be highly nonlinear, with climate-yield correlations even changing signs in response to climate extremes such as floods and droughts, or through multiple impact pathways involving climate related pest and disease outbreaks. Climate variability in some regions may be dominated by non-climate related socio-economic factors, such as migration, conflict, market prices and technology developments. Lastly, but importantly, yield (and possibly climate) data quality may quite simply lack the accuracy to reveal the true climate signal.

Attempting to determine the more coherent signals, it appears that in northeast, northwest and southwest China, rainfall is a limiting factor with yield positively correlated ($p < 0.1$) with this variable. Temperature is negatively related ($p < 0.1$) with seasonal mean yield in the far northeastern and southwestern zones, while positively correlated ($p < 0.1$) in the central regions. As shown by Tian et al. (2011) from a field warming experiment performed in Nanjing of Jiangsu Province, China, a slight warming (0.9 to 1.5°C) increased the plant height, flag leaf area, total green leaf area and the effective tillers, while decreasing the ineffective tillers, and consequently increased wheat yield. Northeast, northwest and southwest China are located in the arid to semi-arid regions, and rain-fed agriculture in these regions dominates; therefore, drought and warming have a significant potential negative impact on crop yield. In these grid cells, >25% of the variability in observed wheat yield can be explained by the inter-annual variability in seasonal total precipitation and mean temperature.

In contrast, in the North China Plain and southeast China, there is a large swathe where observed wheat yield is negatively correlated with the total amount of seasonal rainfall. The North China Plain and southeast China are semi-humid/humid (but suffer from climate extremes of flooding and drought) and irrigated agriculture accounts for a large fraction in this region, mitigating the effect of interannual precipitation variability. Here yield is more likely to be restricted by more extreme water related events, such as waterlogging resulting from flooding or water-related diseases and pests.

3.1.2. Modelled relationship

The seasonal climate–yield relationships can be reproduced using a yield generated by the dynamical crop model GLAM driven by daily climate data (Fig. 4). In a 'perfect model' and 'perfect climate data' scenario, this exercise would reveal where one could expect to find correlations between seasonal climate and yield data. As expected, the regions for which a significant correlation ($p < 0.1$) between seasonal anomalies of climate and yield exist (in 904 out of 1238 grid cells) are more widespread, possibly indicating the questionable reliability of the observed yield data. However, a third (27%) of the grid cells still do not produce a statistically significant correlation over the 16 yr period. This highlights the highly non-linear nature of climate–yield relationships. It is emphasized that in these model integrations, the only factors that change from year to year are the climate drivers. Moreover, nonlinear impacts of climate extremes such as low temperature, frosts, hail, flooding and pest outbreaks are not included in the model.

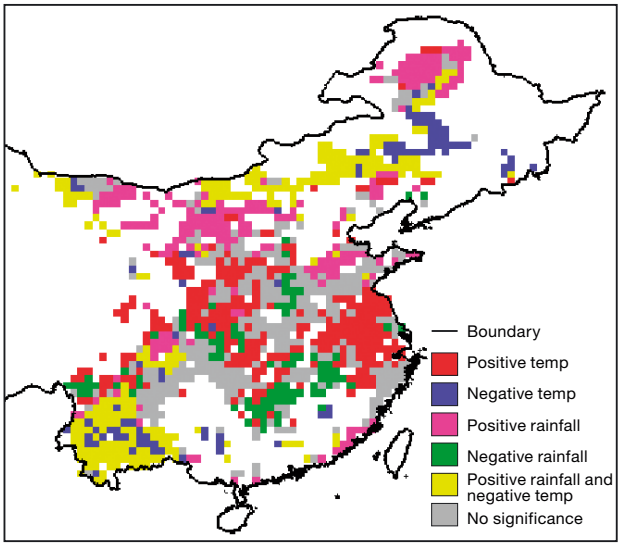

Fig. 4. As Fig. 3 but instead using the modelled yield produced by GLAM driven with the rainfall and temperature observations

The model yield results in general reveal a strong negative correlation with temperature in southwestern China where wheat yields are limited by high temperatures, with the same relationship also observed in the far northeast. The same correlations were hinted at in the observed yields, increasing confidence in the dynamical model simulations. Increases in rainfall benefit the modelled yield across the non-irrigated regions of northeast, northwest and southwest China, again not in disagreement with the observations. The largest discrepancy between using modelled or observed yields occurs in the centre and east of China, for which the modelled yield is dominated by a positive correlation with temperature, which is barely hinted at when using observed yields. In GLAM, the increase in temperature advanced the development stages of winter wheat in some grid cells; hence, lower temperatures (sub-optimal or no-stress) were experienced during the leaf expansion and grain-filling periods. Thus, the lengths of leaf expansion and grain-filling were extended, with corresponding increases in leaf area index (LAI), and biomass and yield accumulation (Li et al. 2010b). Moreover, in the east of China the large-coherent signal of negative correlation with precipitation is lacking when using modelled yield. This points to the need to add a treatment for waterlogging and flooding in the dynamical model, which is presently neglected.

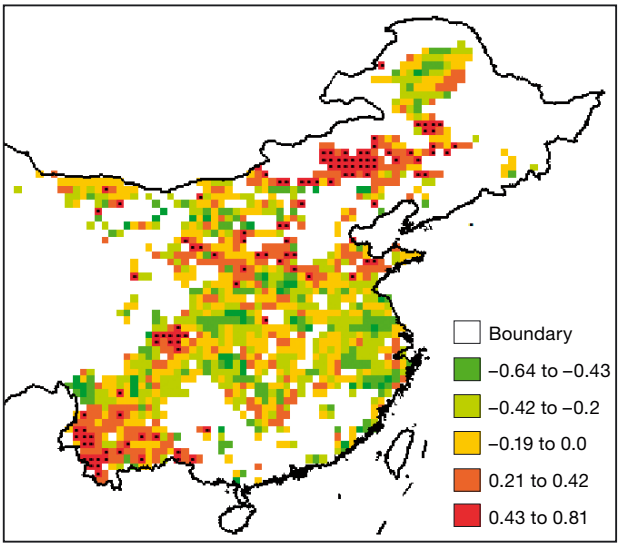

Fig. 5. Correlation coefficients between simulated and observed original yield at the 0.5° scale in China from 1985 to 2000. For r > 0.425, correlation is significant at the 10% significance level (grid cells with dots)

In summary, apart from the east of China affected by flooding, the dynamical model shows some broad agreement with the observed statistical climate–yield relationships. However, the latter are spatially very noisy, and in the majority of locations sub-seasonal variability and other factors confound the climate–yield relationship.

3.2. Model skill for regional aggregated yield

Fig. 5 shows the correlation coefficients between simulated and observed original yield at the 0.5° scale in China from 1985 to 2000. If a point-wise correlation between modelled and observed yield is examined as a metric of the skill of the model yield prediction, only 117 out of 1238 grid cells are significant with $p < 0.1$ (Fig. 5). In order to reveal the broad underlying skill of the model predictions, it is therefore necessary to aggregate the simulated and observed yield values from the underlying 0.5° grid to the 5 major regional levels. Only the wheat yield from grid cells with an arable land percentage >50% were used in this process, with the area of arable land derived from the Food and Agriculture (FAO) land cover database (www.fao.org/geonetwork/srv/en/main.home).

The correlation coefficients between observed and simulated wheat yield varied among different regions. There was a poor relationship between simulated and observed yields in the North China Plain and southeast China (Table 2). In these 2 regions the interannual variability in observed wheat yield may be less affected by climate variability due to a larger proportion of irrigation (Fig. 2), which, as stated earlier, is not represented in these model integrations. In the rain-fed agricultural regions such as northeast, northwest and southwest China, there is a significant correlation between observed and simulated at the 5% significance level (Table 2). The GLAM was able to capture a large fraction of interannual variability in the observed yields in these 3 regions (Fig. 6). The GLAM model gave a better fit of simulated yield in the rain-fed agriculture dominant regions than irrigation-dominated regions in China, as expected due to the fact that irrigation reduces the dependence on year to year rainfall fluctuations, leaving temperature and radiation as the main climatic drivers of yields in non-flood years.

3.3. Sensitivity to sub-seasonal temporal scale

In order to demonstrate the importance of sub-seasonal variability of climate variables, a set of integrations was made in the dynamical crop model with the driving climate variables (station gauge data) in turn averaged over 5, 10 and 30 d to progressively filter out short term variability.

Table 2. Mean observed (obs) and simulated yield (mean ± SD), and correlation coefficient (between obs and simulated) 1985–2000, in northeast, northwest, southeast and southwest China and the North China Plain (NCP), climate data aggregated from fine (0.5°) to coarse (1° and 2°) resolution grids. Significant correlation: $^{*}p < 0.05$, $^{**}p < 0.01$

	Mean yield (kg ha^{-1})				Correlation		
	obs	0.5°	1°	2°	0.5°	1°	2°
Northeast	1904 ± 279	1904 ± 335	1712 ± 305	1698 ± 304	0.595*	0.551*	0.455
Northwest	1862 ± 155	1652 ± 229	1698 ± 195	1693 ± 197	0.712**	0.684**	0.508*
NCP	3207 ± 183	3022 ± 334	3050 ± 312	3055 ± 293	0.090	−0.113	−0.131
Southeast	1718 ± 66	1670 ± 168	1672 ± 170	1670 ± 172	−0.333	−0.265	−0.242
Southwest	1712 ± 99	1597 ± 201	1614 ± 171	1612 ± 170	0.516*	0.339	0.351

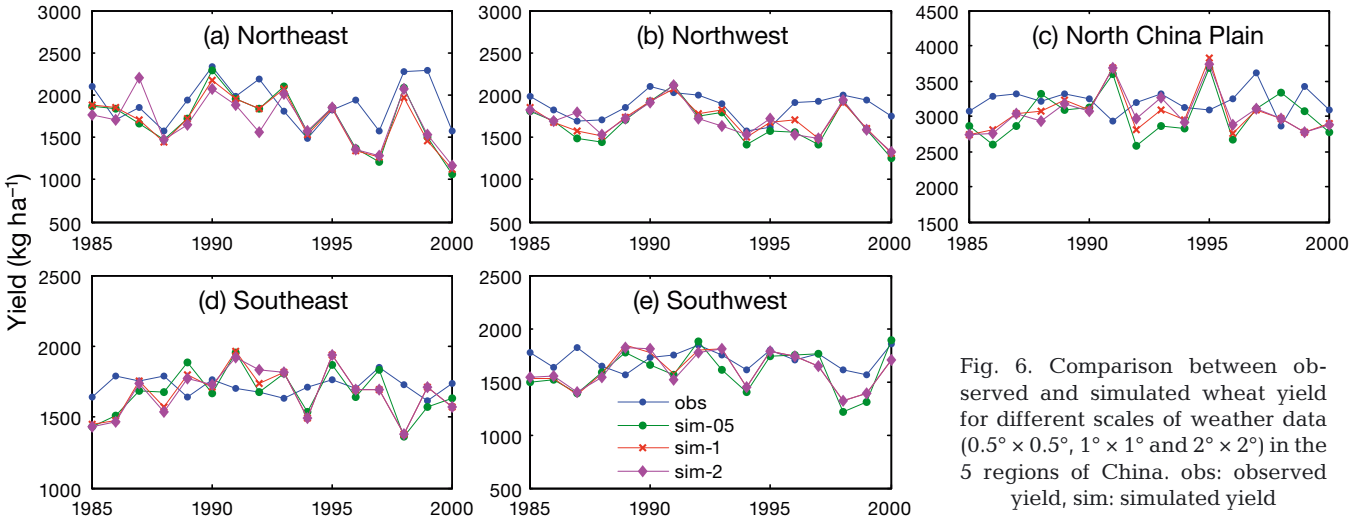

Fig. 6. Comparison between observed and simulated wheat yield for different scales of weather data (0.5° × 0.5°, 1° × 1° and 2° × 2°) in the 5 regions of China. obs: observed yield, sim: simulated yield

In the first set of experiments, daily maximum and minimum temperature and solar radiation are used and the averaging is applied to the rainfall. Fig. 7 shows the comparison of simulated wheat yield from GLAM using daily, 5, 10 and 30 d average values for rainfall. Results show that using pentad averages of rainfall, variability in simulated yield is very similar to that using the original daily dataset for the selected sites in China, although in the semiarid sites such as Guyuan (36.00° N, 106.27° E) and Huma (51.72° N, 126.65° E) there is reduced wheat yield in some years because averaging the daily rainfall over time may bias the daily rainfall toward lower values below the threshold of drought stress and consequently reduce LAI and crop transpiration while increasing evaporation (as showedn Fig. 8). Overall, the mean simulated yield with pentad rainfall is not significantly different to that produced with the daily dataset (Table 3).

Driving GLAM with 10 d average rainfall produces similar interannual variability in yield as using the original daily dataset at all sites (Fig. 7). However, the mean yield was significantly different from that simulated using daily rainfall in 2 semi-arid sites of spring wheat (Table 3). Extending the averaging period further to monthly (30 d) averaging timescales results in large differences in simulated mean yield and yield variability compared with using the original daily rainfall in the most of the selected sites in

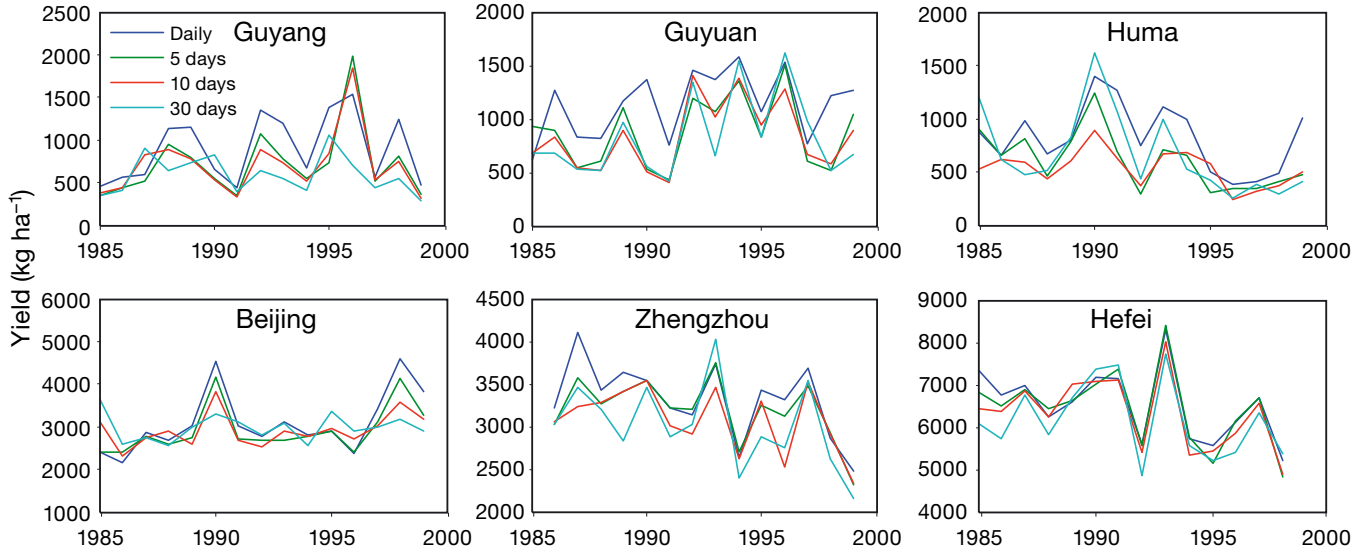

Fig. 7. Comparison between simulated wheat yields from GLAM using daily weather data and simulated yield when 5, 10 and 30 d average values for rainfall were used

Table 3. Two-sample Kolmogorov–Smirnov (KS) test p-values for simulated wheat driven by daily weather data against simulations driven by 5, 10 and 30 d rainfall and temperature, respectively. *p < 0.05

Locations	Rainfall			Temperature		
	5 d	10 d	30 d	5 d	10 d	30 d
Guyang	0.136	0.136	0.051	0.998	0.89	0.89
Guyuan	0.136	0.051	0.017*	0.89	0.89	0.589
Huma	0.308	0.017*	0.136	0.89	0.89	0.998
Beijing	0.136	0.89	0.89	0.998	0.998	0.89
Zhengzhou	0.862	0.267	0.111	0.267	0.267	0.012*
Hefei	0.997	0.862	0.541	0.997	0.541	0.267

China (Fig. 7). It indicates that crop yield is affected not only by the growing seasonal total amount of rainfall but also by the distribution of sub-seasonal rainfall because water stress or excessive soil water at a critical growth stage can also cause a significant reduction in crop yield.

These results demonstrate the significant impact sub-seasonal variability of rainfall has on seasonal crop yield, which in many regions is more significant than the interannual variability of the mean rainfall, thus confounding the possibility of applying statistical yield models. When using the average rainfall data, in some cases the times of the rainfall rather than the amount are important for determining the crop yields. This is particularly the case in the arid to semi-arid sites, where simulated crop yield is more sensitive to rainfall variability than the semi-humid to humid sites (e.g. Guyuan) because of the larger variation in temporal distribution and frequency of seasonal rainfall.

A secondary but important conclusion of this comparison is the implication that dynamical models can be integrated for past periods using pentad rainfall data observed from satellites such as the GPCP product (Huffman et al. 1995, 2001), available from 1979.

The averaging experiments were repeated for the temperature variable, with daily rainfall and solar radiation used in each case (Fig. 9). The use of averaged temperature over 5 and 10 d in GLAM has a minor effect compared with simulations using daily temperature (Table 3) at all sites. Only the use of a 30 d running mean had any noticeable impact on the yield variability. This is as expected since temperature is a continuous 'smooth' variable, and it is only when the averaging period exceeds the length of critical period in the crop growth cycle, such as the flowering season, that the averaging has an impact.

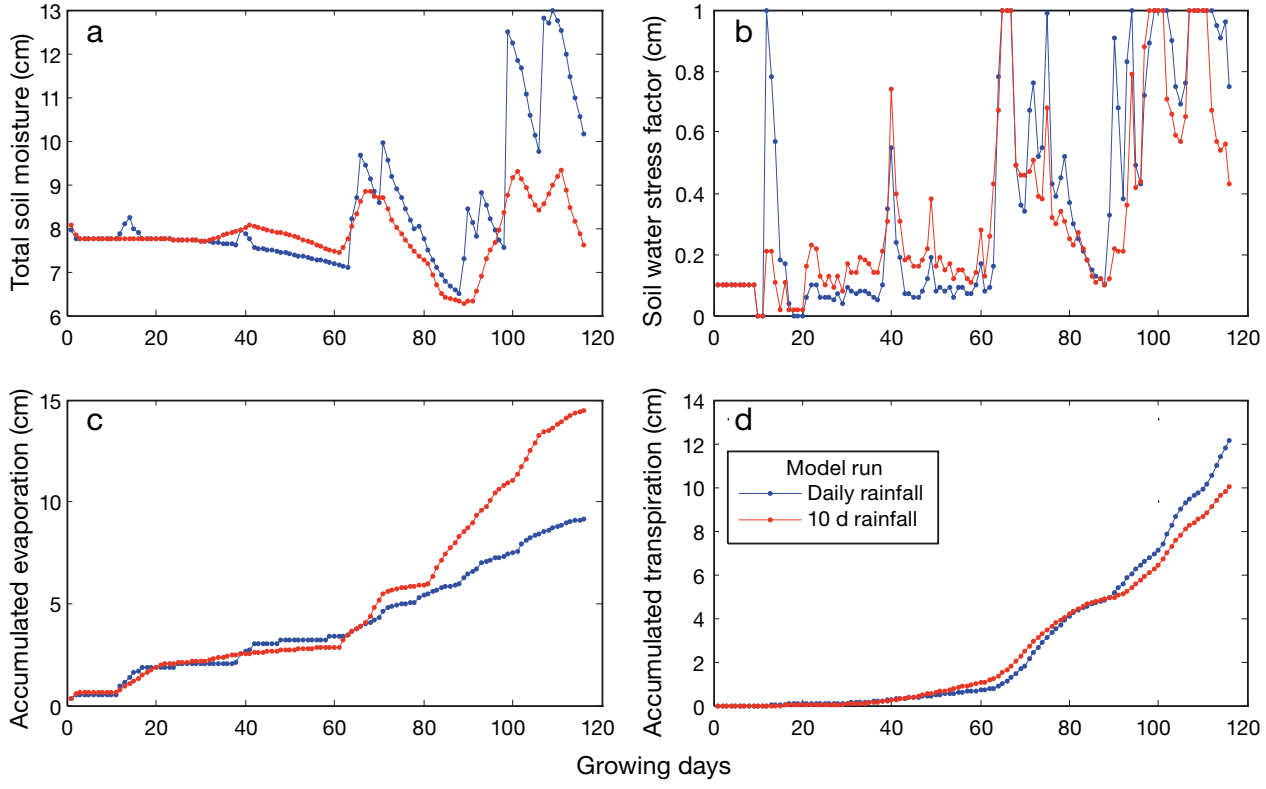

Fig. 8. Example of comparison of total soil moisture, water stress factor, accumulated evaporation and accumulated transpiration in 1997 at Guyuan when the GLAM was run with daily and 10 d average rainfall

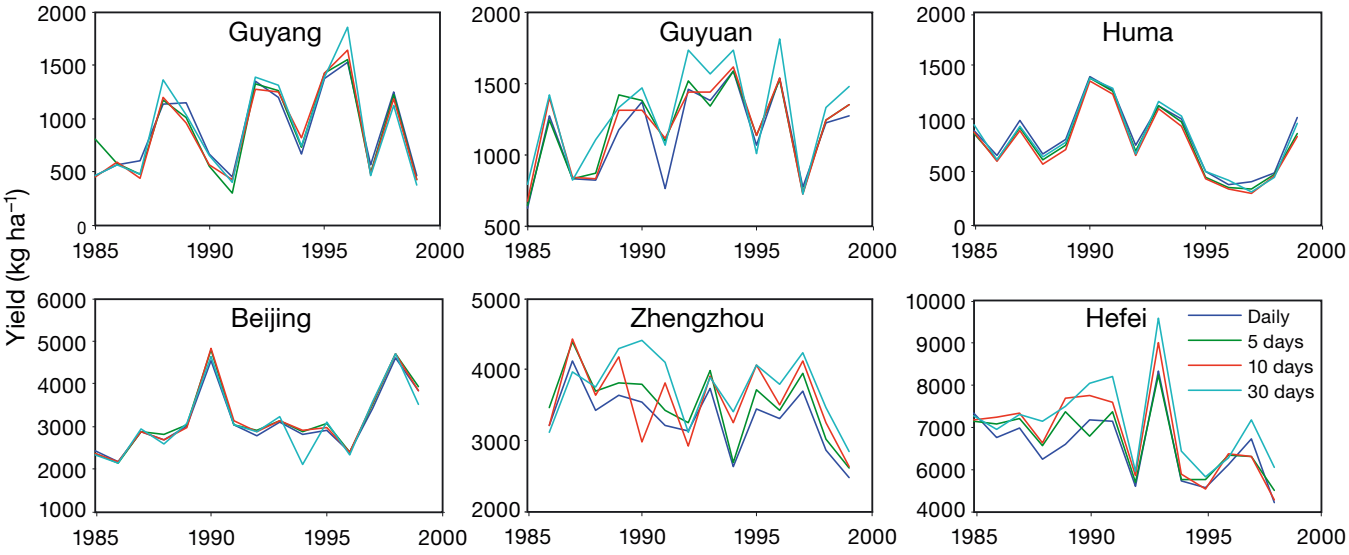

Fig. 9. Comparison between simulated wheat yield from GLAM using daily weather data and simulated yield when 5, 10 and 30 d average values for temperature were used

3.4. Sensitivity to spatial scale

Since rain gauges are unevenly distributed and topography can imply rapidly changing climatic precipitation zones, it is possible that in some regions rain gauges are not representative of the climate in the crop producing zones. Rain gauges are particularly sparse and inhomogeneously distributed in north and western China (see Fig. 1 of Xu et al. 2009). Aggregating rain gauge data across a grid cell may therefore include some irrelevant data that confounds the ability to predict yield.

To illustrate how representative rain coverage in cropping zones are crucial for crop yield monitoring and prediction on a regional level, 2 case studies are shown, in which climate data is taken directly from a number of individual stations that are located close to one another, within a 2° × 2° (called CN2) grid cells. Two grid cells are chosen because they are on rainfed crop areas with a number of individual rain gauges available for public use (in addition to the gridded product): 2 gauges (ref. 53 352 and 53 463) available at the lower rainfall southern grid cell (41° N, 111° E), and 3 gauges used (54 208, 54 102 and 54 115) in a higher rainfall northern grid cell (43° N, 117° E,). GLAM is driven with data from each station and 2° × 2° scale weather data in turn; the resulting simulated yields compared to the 2° × 2° observed regional yield.

The results highlight the importance of spatial variability and selecting representative stations. For example, in the southern test location, driving GLAM with data from one of the stations (53463) leads to a significant correlation of simulated yields to observed yields (Table 4), and yet, using the nearby station number 53 352 results in no correlation with the observed yield. There is high uncertainty in the simulated yield (Fig. 10) when the model is driven by individual station weather data, due to big differences in rainfall, especially in 1990 and 1991 (Fig. 11). Rainfall at the 2 stations differs due to topographical influences, although in some years the correspondence is good (Fig. 11). Assuming that the data quality is similar at both stations, this exercise demonstrates one of the drawbacks of attempting to model yield over coarse regional scales using the station weather data. It would appear in this case, for example, that the agriculturally productive regions within the 2° × 2° grid cell are predominately situated in the subregion whose local climate is more reliably described by Station 53 463.

In many grid areas, of course, both rainfall and cultivated areas are more uniform, and the grid cell (43° N, 117° E) gives such an example. As shown in Table 4 there is a significant ($p < 0.05$) correlation between the observed and simulated yield driven by the 2° × 2° gridded rainfall product and each individual station. Here, rainfall variability between stations was more similar, and uncertainty in simulated yield is small (Fig. 10).

The issue of the appropriate spacial scale of climate data to run a dynamical regional crop model is investigated further. GLAM was run with the gridded climate data at the original 0.5° scale and coarser 1° × 1° and 2° × 2° resolutions. Then the simulated yield was aggregated to regional level respectively. Due to the

Table 4. Correlation coefficients between observed and simulated wheat yields and total seasonal precipitation amounts from 1985 to 2000 using individual stations in addition to gridded product (see Section 2.2 for details). *p < 0.05, **p < 0.01

Gauge no.	Location	Altitude (m)	Rainfall (mm)	r
CN2 point	41° N, 111° E			
CN2	41° N, 111° E,		121	0.65*
53352	41.7° N, 110.4° E	1377	108	0.43
53463	40.8° N, 111.7° E	1063	145	0.67*
Station average			127	0.70*
CN2 point	43° N, 117° E			
CN2	43° N, 117° E		262	0.76**
54102	44.0° N, 116.1° E	990	186	0.70**
54115	43.6° N, 118.1° E	799	236	0.75**
54208	42.2° N, 116.5° E	1245	273	0.74**
Station average			231	0.723**

nonlinearity of yield production as a function of rain rate (r), the regional average yield (Y) will differ in each case since: $\overline{Y(r)} \neq Y(\overline{r})$. However, it is obviously the case that the best agreement with observed yields will be obtained at the highest resolution, since yield data will be subject to random errors that reduce as a function of averaging scale.

The comparison of these integrations reveals that the averaging scale of climate data, has a limited effect on the ability of the model to reproduce mean yield and standard deviation of yield at the 5 regions. Nevertheless, in the rain-fed agricultural regions such as northeast, northwest and southwest China, the model ability to reproduce the inter-annual variability in yields was improved when the GLAM was run with the 0.5° climate data; there is a significant correlation between observed and simulated at the 5% significance level (Table 2). The GLAM was able to capture a large fraction of inter-annual variability in observed yields in these 3 regions. The GLAM driven by the 0.5° resolution of climate data gave a better fit of simulated yield in the rainfed agriculture dominant regions. The model skill in reproducing the observed inter-annual variability of yields decreased when the resolution of climate date was decreased from 0.5° × 0.5° to 1° × 1° and 2° × 2° scales (Table 2).

As shown by Fig. 12, anomalies in the normalized wheat yield at the 0.5° scale in China show frequent isolated data points of opposite sign to the neighbouring areas. If yield data is subject to a variety of factors that contribute to uncertainty, such as sampling errors and macro and micro socio-economic effects, a natural question is whether filtering can be applied to isolate a climate related driver of yield variability in data from other effects. An example of this already in use is the common practice of removing long term upward trends in yield data, attributing these to technology and management practice improvements. Such filters can never be applied unambiguously; long term technology trends may be amplified or offset by climate change temperature trends for example, which must be isolated if climate change impact on yield is the object of the research. In a first attempt, a simple low pass kernel filter was designed to reject crop yield data that was found to be a statistical outlier (using Grubb's test) relative to the surrounding array of 7 × 7 observations, replacing these outliers with the mean yield of the surrounding points. However, the observations filter did not lead to a statistically significant improvement in the agreement between GLAM simulated yields and observations. It is thus likely that an improved filtering technique that identifies spatial scales of climate anomalies, perhaps using an empirical orthogonal function based approach, may be necessary in future studies.

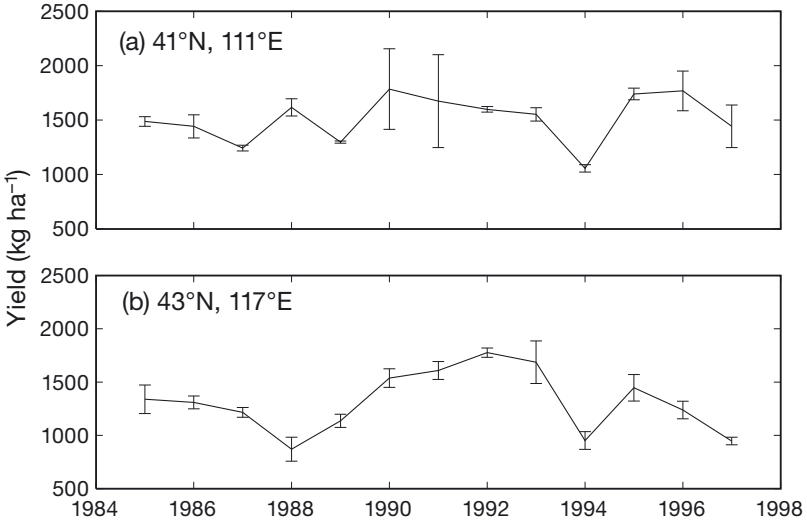

Fig. 10. Error of simulated wheat yield when GLAM was run with individual station weather data in specific grid cells containing multiple climate stations from 1985 to 2000

4. CONCLUSIONS

In order to improve crop forecasting using model-based forecasting systems, it is important to understand the response of crop to climate anomalies relative to other non-climatic drivers of yield, and in particular, over which

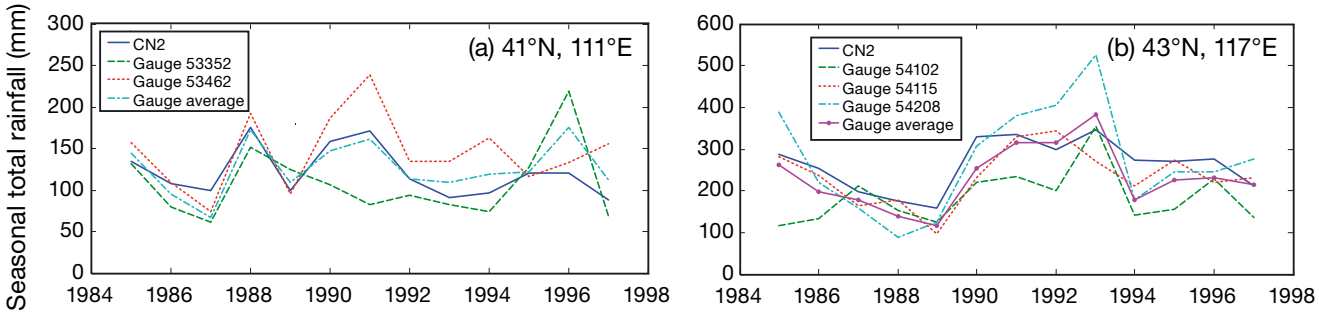

Fig. 11. Sub-sampling of rainfall in specific grid cells with good coverage stations from 1985 to 2000

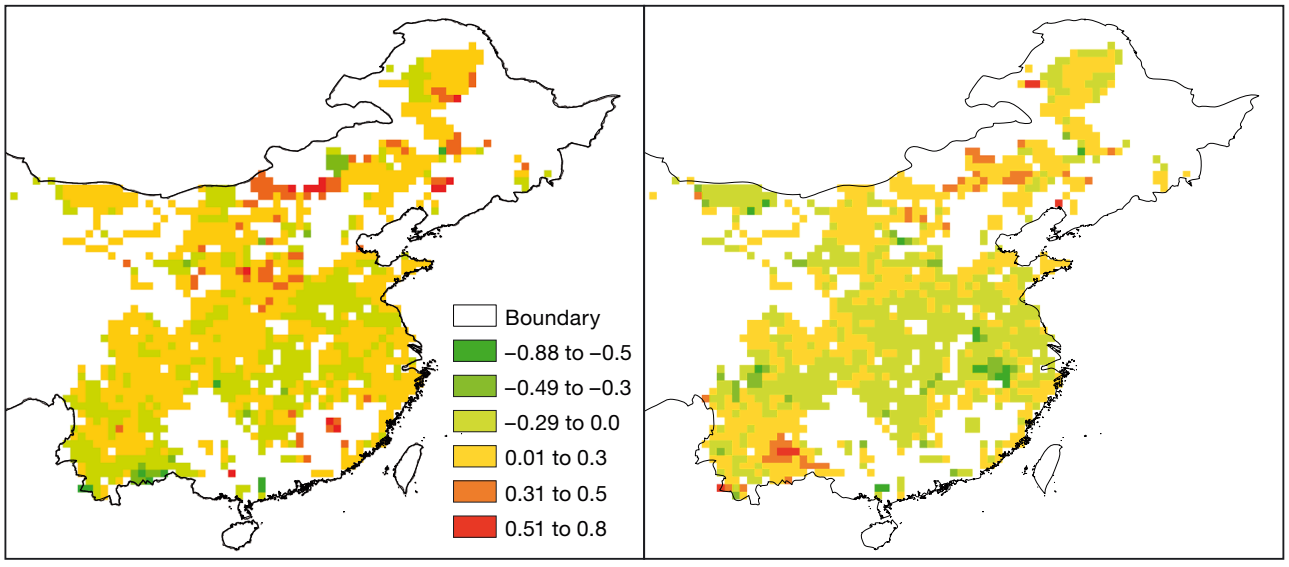

Fig. 12. Anomalies in the normalized wheat yield at the 0.5° scale in China 1985 (left), 1990 (right)

spatial and temporal scales these drivers operate. Using gridded wheat yield data from across China in combination with daily observed ground station data for precipitation and temperature, it was found that a surprisingly limited proportion of locations (just over one half) showed any significant correlation (measured at the 90% level) at all between seasonal anomalies in climate and crop yield. This proportion fell well below one half if a more stringent 95% significant level was used. This analysis immediately reveals the importance of confounding factors. For example management decisions are determined by economic and social factors, pests and diseases, which can lead to highly non-linear climate–yield relationships. Causes for these nonlinearities range from sub-seasonal variations in climate that are neglected in a simple statistical approach, to interacting effects of temperature and rainfall variability, and to straightforward (but difficult to isolate and correct for) random sampling errors and mean biases in both climate and yield data. This highlights the difficulties in using simple statistical yield forecasting tools.

To highlight the importance of the nonlinearities, the same statistical analysis was repeated but with the yield observations replaced by the output from a dynamical model driven by the daily temperature and rainfall observations, supplemented by radiation data from reanalysis. While the use of a model naturally introduces the element of model error due to the uncertainty in the representation of the plant physiology, the model represents the basic physics of the nonlinear relationship between climate and plant growth, and the subsequent yield, and it also takes into account differences in sub-seasonal variability of climate from year to year, since it is integrated on a daily timestep. Even though the climate variables are the only factors that affect yield in the model — which neglects year to year variability due to management decisions and pest/diseases — a statistical analysis of the model output fails to find a significant univariate

or bivariate correlation between yield anomaly and temperature/rainfall variables in around one quarter of the modelled domain in China.

Some of the nonlinear effects were isolated by the application of simple temporal and spatial filtering (averaging). Averaging the precipitation data to 5 d had a limited effect on the modelled yield due to the memory effect of the soil and the resilience of plants to limited water stress. This is a useful result since all currently available daily satellite retrievals for precipitation are only available for approximately the last decade; retrieval techniques applied to the period of the 1980s and 1990s relied heavily on infrared information and thus are only available for pentads or dekad averages due to the necessity to average out sampling errors. Averaging rainfall to dekads already had a large effect on yield, highlighting the importance of sub-dekad dry spells in determining seasonal mean yield, and this was even more the case with the application of monthly averaging. For temperature, the effect was smaller, as expected, since temperature is a more smoothly evolving variable; nevertheless, monthly averaging had a significant effect.

Spatially averaging the driving climate data shows that best agreement with observed yields is obtained at the highest resolution. The GLAM model driven by the 0.5° resolution of climate data gave a better fit of simulated yield in the regions dominated by rainfed agriculture. However, in the regions dominated by irrigation, the model performance appears very poor. Again there are many possible reasons for this, with some of the confounding factors above compounded by neglected or incorrect model physics. For example, in the eastern Chinese region, modest drought is mitigated by a high proportion of irrigation, and while the dynamic model used in the study has the ability to represent irrigation, it could not be employed in the study due to the lack of available information concerning the specific irrigation regions and application practices. Moreover, in these regions, the dominant relationship is in fact a negative one between rainfall and yield, which results from a few years of catastrophic flooding. Research has shown that waterlogging has a negative effect on crop yield, mainly by reducing transpiration and root growth (Hu et al. 2004). The dynamic crop model does not currently incorporate a representation of the negative effect of waterlogging on transpiration, root growth and eventual yield; thus a companion paper to this one will introduce such a component to the model.

Our results show the need for the development of a filtering technique to reduce sampling noise and also isolate the climate signal in the yield data from other effects. It is not clear what the best approach to this should be. This study attempted a very simple application of spatial averaging of climate data to average out sampling errors, but this deteriorated the modelled yield skill due to the subsequent loss of local climatic information. A case study of isolating individual station data showed that in some regions very small-scale spatial variability was highly relevant, with stations only tens of km distant from the main cropping areas being irrelevant for the calculation of yield, while others stations showed high skill. We also attempted to apply statistical tests to isolate small scale variability in the yield data due to non-climatic factors, e.g. using Grubb's test for statistical outliers, but this was not found to greatly improve the overall model agreement with the filtered data. Thus research is currently underway to determine if an improved filtering approach — possibly based on the use of empirical orthogonal functions to identify associated large-scale modes of seasonal climate variability also present in the yield data — can be developed that can improve the present performance of the dynamical crop modelling system, which can then ultimately be applied using seasonal climate forecasts in place of the observational data used in the present study.

Ackowledgements. This work is supported by a grant from the Italian Ministry of Foreign Affairs (MAE grant 241.FITU 11 G), the National Basic Research Program of China (973 Program, No. 2012CB955904) and the National Basic Research Program of China (project No. 2010CB951504).

LITERATURE CITED

Batjes NH (1997) A world dataset of derived soil properties by FAO-UNESCO soil unit for global modelling. Soil Use Manage 13:9–16

Becker-Reshef I, Vermote E, Lindeman M, Justice C (2010) A generalized regression-based model for forecasting winter wheat yields in Kansas and Ukraine using MODIS data. Remote Sens Environ 114:1312–1323

Bezuidenhout CN, Singels A (2007) Operational forecasting of South African sugarcane production. 2. system evaluation. Agric Syst 92:39–51

Bouman B, Diepen C, Vosen P, van Der Wal T (1995) Simulation and system analysis tolls for crop yield forecasting. In: Teng PS, Kropff MJ, ten Berge HFM, Dent JB, Lansigan FP, Van Laar HH (eds) Application of systems approaches at the farm and regional levels, Vol. 1. Kluwer, Dordrecht, p 325–340

Bowman KP (2005) Comparison of TRMM precipitation retrievals with rain gauge data from ocean buoys. J Clim 18:178–190

Challinor AJ, Wheeler TR, Craufurd PQ, Slingo JM, Grimes

DIF (2004) Design and optimisation of a large-area process-based model for annual crops. Agric For Meteorol 124:99–120
Challinor AJ, Wheeler TR, Craufurd PQ, Slingo JM (2005) Simulation of the impact of high temperature stress on annual crop yields. Agric Meteorol 135:180–189
Ciach GJ (2003) Local random errors in tipping-bucket rain gauge measurements. J Atmos Ocean Tech 20:752–759
CSY (ed) (2001) China statistical yearbook, Vol. 2001. China Statistical Press, Beijing
Cui D, Liu H, Min J (1983) Main crops climate resources atlas in China. Meteorology Press, Beijing
Dee DP, Uppala SM, Simmons AJ, Berrisford P and others (2011) The era-interim reanalysis: configuration and performance of the data assimilation system. Q J R Meteorol Soc 137:553–597
Easterling WE, Weiss A, Hays CJ, Mearns LO (1998) Spatial scales of climate information for simulating wheat and maize productivity: the case of the US Great Plains. Agric For Meteorol 90:51–63
Grimes DIF, Pardo-Iguzquiza E, Bonifacio R (1999) Optimal areal rainfall estimation using raingauges and satellite data. J Hydrol (Amst) 222:93–108
Hannaford J, Lloyd-Hughes B, Keef C, Parry S, Prudhomme C (2011) Examining the large-scale spatial coherence of European drought using regional indicators of rainfall and streamflow deficit. Hydrol Processes 25:1146–1162
Hansen JW, Potgieter A, Tippett MK (2004) Using a general circulation model to forecast regional wheat yields in northeast Australia. Agric For Meteorol 127:77–92
He ZH, Rajaram S, Xin ZY, Huang GZ (2001) A history of wheat breeding in China. CIMMYT, Mexico City
Hu JC, Cao WX, Zhang JB, Jiang D, Feng J (2004) Quantifying responses of winter wheat physiological processes to soil water stress for use in growth simulation modeling. Pedosphere 14:509–518
Huffman GJ, Adler R, Rudolph B, Schneider U, Keehn P (1995) Global precipitation estimates based on a technique for combining satellite-based estimates, rain gauge analysis, and NWP model precipitation information. J Clim 8:1284–1295
Huffman GJ, Adler RF, Morrissey MM, Bolvin DT and others (2001) Global precipitation at one-degree daily resolution from multi-satellite observations. J Hydrometeorol 2: 36–50
Jones JW, Hansen JW, Royce FS, Messina CD (2000) Potential benefits of climate forecasting to agriculture. Agric Ecosyst Environ 82:169–184
Joyce RJ, Janowiak JE, Arkin PA, Xie P (2004) CMORPH: a method that produces global precipitation estimates from passive microwave and infrared data at high spatial and temporal resolution. J Hydrometeorol 5:487–503
Li S (2008) Investigating the impacts of climate change on wheat in China. PhD thesis, University of Reading
Li S, Wheeler TR, Challinor AJ (2007) Development of a large area wheat crop model for studying climate change impacts in China. J Agric Sci 145:47
Li S, Wheeler TR, Challinor AJ, Lin ED, Ju H, Xu YL (2010a) The observed relationships between wheat and climate in China. Agric For Meteorol 150:1412–1419
Li S, Wheeler TR, Challinor AJ, Lin ED, Xu YL, Ju H (2010b) Simulating the impacts of global warming on wheat in China using a large area crop model. Acta Meteorol Sin 24:123–135
Nemecek T, Derron JO, Roth O, Fischlin A (1996) Adaptation of a crop-growth model and its extension by a tuber size function for use in a seed potato forecasting system. Agric Syst 52:419–437
Olesen JE, Boher PK, Jensen T (2000) Comparison of scales of climate and soil data for aggregating simulated yields of winter wheat in Denmark. Agric Ecosyst Environ 82: 213–228
Porter JR, Semenov MA (1999) Climate variability and crop yields in Europe. Nature 400:724
Porter JR, Semenov MA (2005) Crop responses to climatic variability. Philos Trans R Soc Lond B Biol Sci 360: 2021–2035
Semenov MA, Porter JR (1995) Climatic variability and the modeling of crop yields. Agric For Meteorol 73:265–283
Sudduth KA, Drummond ST (2007) Software for removing errors from crop yield maps. Agron J 99:1471–1482
Thorne V, Grimes D, Dugdale G (2001) Comparison of TAMSAT and CPC rainfall estimates with raingauges, for southern africa. Int J Remote Sens 22:1951–1974
Thornton PK, Bowen WT, Ravelo AC, Wilkens PW, Farmer G, Brock J, Brink JE (1997) Estimating millet production for famine early warning: an application of crop simulation modelling using satellite and ground-based data in Burkina Faso. Agric For Meteorol 83:95–112
Tian YL, Chen J, Deng XA, Zheng JC, Zhang WJ (2011) Effects of asymmetric warming on the growth characteristics and yield components of winter wheat under free air temperature increased. Chin J Appl Ecol 22:681–686
Villarini G, Mandapaka PV, Krajewski WF, Moore RJ (2008) Rainfall and sampling uncertainties: a rain gauge perspective. J Geophys Res 113:D11102
Xie PP, Arkin PA (1997) Global precipitation: a 17-year monthly analysis based on gauge observations, satellite estimates, and numerical model outputs. Bull Am Meteorol Soc 78:2539–2558
Xie P, Yatagai A, Chen M, Hayasaka T, Fukushima Y, Liu CM, Yang S (2007) A gauge based analysis of daily precipitation over East Asia. J Hydrometeorol 8:607–626
Xu Y, Gao X, Shen Y, Xu C, Shi Y, Giorgi F (2009) A daily temperature dataset over China and its application in validating an RCM simulation. Adv Atmos Sci 26:763–772

Editorial responsibility: Gerrit Hoogenboom, Prosser, Washington, USA

Submitted: October 24, 2011; Accepted: June 2, 2012
Proofs received from author(s): November 5, 2012